MAUSAM, **56**, 1 (January 2005), 97-106

551.577.31 : 551.465.531

Diurnal and intraseasonal variations observed on the West Coast of India

G. S. BHAT, PRASHANTH L. RAO, V. G. SANGOLLI,
G. P. BHAT*, A. B. CHANDELKAR**, H. RAO*** and V. B. KADAV****
Indian Institute of Science, Bangalore, India
**India Meteorological Department, Karwar, India*
***Regional Fruit Research Center, Vengurla, India*
****India Meteorological Department, Honnavar, India*
*****Mango Research Center, Vijaydurg, India*
e mail : bhat@caos.iisc.ernet.in

सार – अरब सागर मानसून प्रयोग (आरमेक्स) के कार्य के रूप में भारत के पश्चिमी तट पर अनेक स्वचालित मौसम स्टेशन स्थापित किए गए और उनमें से कुछ स्टेशन एक वर्ष से भी अधिक समय से मौसम संबंधी आँकड़ें रिकार्ड कर रहे हैं। इस शोध–पत्र में तीन तटीय स्टेशनों नामतः होनावर, कारवाड और विजयदुर्ग में जुलाई 2002 से दिसंबर 2003 के दौरान लिए गए स्थानिक परिवर्तन प्रस्तुत किए गए हैं। वायु तापमान, आर्द्रता, पवन गति आदि में मौसमी परिवर्तन आशानुरूप पाए गए हैं। वर्षा के पैटर्न में दैनिक परिवर्तन प्रबल रूप से देखा गया है किंतु होनावर ओर विजयदुर्ग, जिन दोनों के बीच की दूरी 250 कि.मी. से अधिक नहीं हैं, के स्थानीय समय पर निर्भरता भिन्न है। इससे यह पता चलता है कि पूरे वर्ष में विभिन्न समयों के मान में धरातल का दाब प्रबल परिवर्तन दर्शाता है तथा प्रमुख समय के माप मौसमों के साथ बदलते हैं।

ABSTRACT. As part of the Arabian Sea Monsoon Experiment (ARMEX), several automatic weather stations (AWSs) were installed on the west coast of India, and some among them have been recording weather data for more than one year. Here temporal variations observed at three coastal stations, namely Honnavar, Karwar and Vijaydurg during July 2002 to December 2003 are presented. The seasonal variations in air temperature, humidity, wind speed, etc., are along the expected lines. A strong diurnal variation in rainfall pattern is observed, but the dependence on local time is different at Honnavar and Vijaydurg which are not more than 250 kilometres apart. It is shown that the surface pressure exhibits strong variations on different time scales throughout the year, and the dominant time scales shift with the seasons.

Key words – ARMEX, Coastal weather, Monsoon, Diurnal variations, AWS, Seasonal variations, Surface observations.

1. Introduction

During the summer monsoon, the Indian west coast receives heavy rainfall in the latitudinal belt between 11° N and 20° N. Areas where the June-September average exceeds 250 cm hugs the coast and is limited to the windward side of the Western Ghats (Rao, 1976). Both orography and dynamics play a crucial role here. Major contribution to the seasonal rainfall comes from few active spells, during which period the rainfall may exceed 20 cm day^{-1} at some stations. These intense rainfall events (IREs) can cause flooding, land slides and disrupt normal life. It is believed that the development of an offshore trough (OST) is important in producing IREs however, the precise nature of OST including its spatio-temporal structure are yet to be documented. Therefore in the Arabian Sea Monsoon Experiment (ARMEX), OST and the west coast monsoon rainfall were given due importance. It is believed that the weather systems responsible for IREs are intense mesoscale vortices. To delineate their structure, high spatio-temporal resolution data are required. In order to improve the spatial coverage in the study area, 10 **A**utomatic **W**eather **S**tations (AWS) were installed along the west coast of India as part of the ARMEX programme. The primary purpose of these AWSs was to provide continuous surface data (every 10 minutes or so) during the ARMEX field phases.

TABLE 1

Variables measured and the make of the sensors/instruments in the automatic weather station installed by IISc

S. No.	Variable/Instrument	Make	Measuring Range	Measurement height
1	Temperature & humidity	ROTRONICS, MP100H with Hygroclip S3 in R. M. Young radiation shield	Temp : –40 to +60° C RH : 0 to 100 %	2 m
2	Pressure	VAISALA, Barometer PTA100	800 to 1060 hPa	1.2 m
3	Wind speed & direction	R. M. YOUNG, Wind Monitor – Marine model 05106-5	Wind dir : 0 to 360° Wind speed : 0 to 60 m/s	4 m
4	Rain gauge	R. M. YOUNG, Tipping bucket, model 52203	0.1mm resolution	1 m
5	Data logger	Campbell model CR10X	-	-

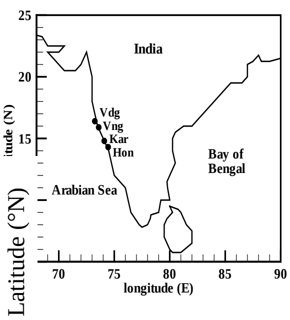

Longitude (°E)

Fig. 1. Locations of automatic weather stations installed by IISc on the west coast of India. Hon – Honnavar, Kar – Karwar, Vng – Vengurla, Vdg – Vijaydurg

Indian Institute of Science, Bangalore was given the task of installing AWSs at Honnavar (14° 17′ N & 74° 27′ E) and Karwar (14° 47′ N & 74° 08′ E) in Karnataka, and Vengurla (15° 52′ N & 73° 38′ E) and Vijaydurg (16° 23′ N & 73° 15′ E) in Maharashtra (Fig. 1). All are coastal stations and climatically favourable locations of IREs. These AWSs have been kept operational beyond the ARMEX field phase and weather data records for more than a year are available now. The present study is based on the data collected at the above 4 stations. The study describes the installation and operation of AWSs. This is followed by seasonal, diurnal and intraseasonal variations observed during the year 2003. The daily rainfall values from AWS and India Meteorological Department (IMD) rain gauges are compared. The agreement between the two is generally good.

2. AWS installation and instrumentation

At the stations selected for installing AWSs, it is difficult to find a place that can really meet the ideal site requirements. Safety of the instruments and the availability of electricity (to run PCs for downloading data and charging battery) are other important considerations. After inspecting the sites, it was decided that the spots where IMD is presently collecting data are perhaps the best locations for setting up AWSs. At Honnavar and Karwar, AWSs have been installed within the IMD premises. At Vengurla, AWS is in the campus of the Regional Fruit Research Centre, and at Vijaydurg, it is inside the Mango Research Centre, a branch of Regional Fruit Research Centre, Vengurla.

The variables measured at each station included air temperature, humidity, pressure, wind speed, wind direction and rainfall. Being coastal areas, corrosion of sensors/instruments is an important consideration. During the Bay of Bengal Monsoon Experiment (BOBMEX) carried out in 1998-99, instruments suited for application under marine conditions were examined (Bhat and Ameenulla 2000) and the present choice of instruments was guided by this experience. The sensors and the makes

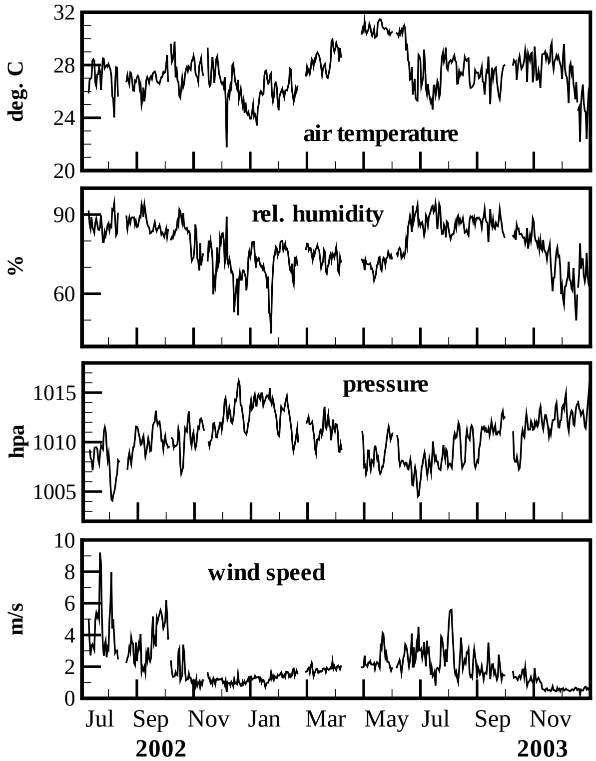

Fig. 2. Time series of daily average values at Karwar from July 2002 – Dec 2003

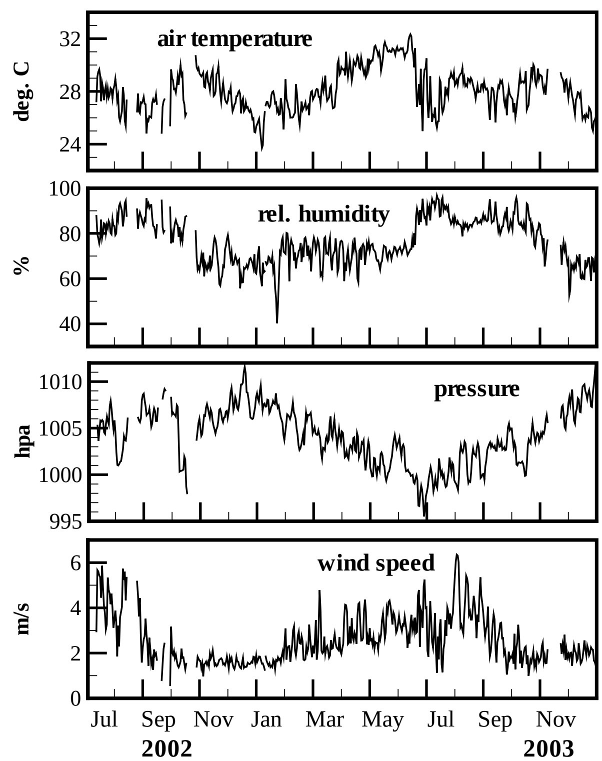

Fig. 3. Time series of daily average values at Vijaydurg from July 2002 – Dec 2003

selected for different measurements and the measurement heights are shown in Table 1. The height of sensor mounting is chosen to be similar to that followed by IMD in their AWS installations. The instruments were fixed on a tower made from stainless steel material so that the tower does not get corroded and lasts for many years. Variables were continuously sampled once every 5 seconds and 10 minute averages were calculated and stored in the data logger memory. The data logger can store about 2 weeks data, and if not downloaded within this time, memory is overwritten resulting in data loss. Data are transferred to a PC normally once a week.

3. Results

(*i*) *Seasonal variations*

The AWSs are in operation since 15 June 2002, however, owing to certain operational problems, data are available from late July 2002 onwards. In Figs. 2 & 3 the time series of daily average air temperature, relative humidity, surface pressure and wind speed are shown at Karwar and Vijaydurg respectively. At these coastal stations, seasonal changes in relative humidity (RH), pressure and wind speed are clearly seen. Air temperature varied in 20° - 32° C range and the amplitude of its annual cycle is found to be comparable to that of the diurnal variation in the winter months. Values of RH are low during November-May period and high (above 80%) during June-September. Wind speeds are very low during November to February. The daily average wind speed shown here is a vector averaged wind speed and not the average of 10 minute averaged wind speeds. The eastward (*u*) and northward (*v*) components of wind vector (*V*) were calculated at each sampling time, and the data logger stored 10 minute averaged *u* and *v* values. Mean wind speed and wind direction are calculated from daily average values of *u* and *v*. This procedure was adapted after noticing large differences between the expected and measured wind directions during certain periods. In particular this happens when the wind blows from north. Suppose the wind direction at one instant is 355° and at another instant 5°. Upon averaging, the resulting wind direction is 180°, which we know is clearly incorrect. Vector averaging overcomes this problem, however, has its limitation. For example, during the post and pre monsoon months, sea breeze circulation is prominent and wind direction almost reverses during certain periods in the day and vector averaged wind speeds are smaller than

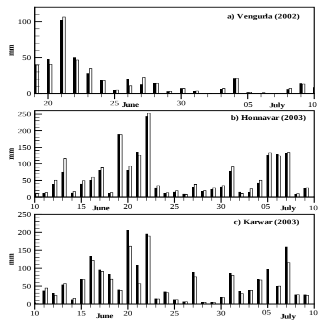

Rainfall

Figs. 4(a-c). Daily rainfall measured by automatic (AWS) and IMD rain gauges. Filled and open bars refer to IMD and AWS rain gauges

the scalar averaged values. Therefore, the average wind speeds shown in Figs. 2 & 3 underestimate the speed with which winds were blowing during the winter months. This can influence the surface heat flux calculations using the bulk algorithms. For example, if sensible and latent heat fluxes are calculated using short time (~20-30 minute) average values, then the resulting daily average values will be larger compared to those based on daily average wind speeds.

It is observed from Figs. 2 & 3 that there are gaps in the time series. Occasionally there were problems with the PC, battery charger and data logger, and some data gaps are due to these. An equal contribution came from not downloading data in time (*i.e.*, the data logger memory was overwritten) and from overwriting a previous data file.

(*ii*) *Rainfall pattern*

The variable of most interest in ARMEX phase I is the rainfall. Figs. 4(a-c) shows typical pattern of daily rainfall at Vengurla, Honnavar and Karwar for some days during June and July. Active and weak spells of rain around the monsoon onset time can be seen in this figure. Notice that during 11 June - 9 July 2003, it rained on all

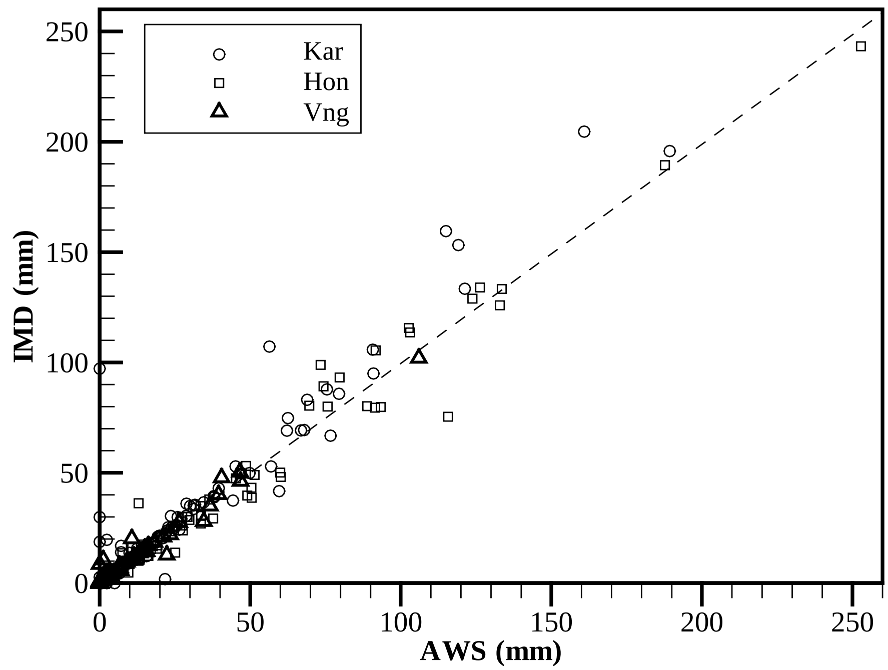

Fig. 5. Scatter plot of AWS *versus* IMD daily rainfall

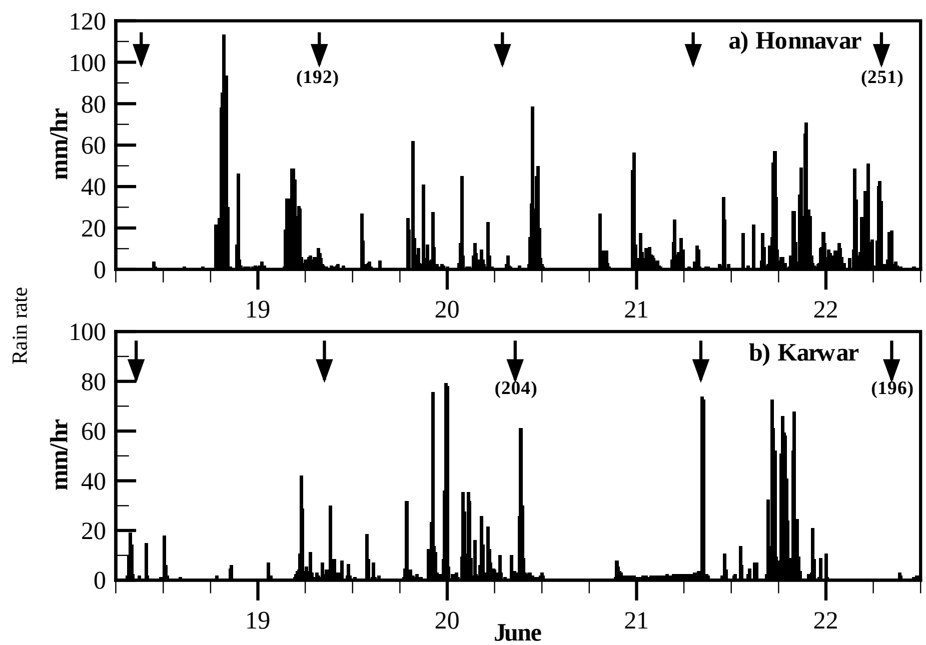

Figs. 6(a&b). Rain rates during the onset stage of monsoon 2003 at (a) Honnavar and (b) Karwar when intense rainfall events took place

days at Honnavar and Karwar. At both places daily rainfall was above 50 mm on about 35% of the days, and near about 200 mm or more on two days. Also shown in Figs. 4(a-c) is the corresponding daily rainfall measured by the IMD rain gauge. AWS rain gauge is a tipping bucket type (Table 1) whereas IMD's is manual type and the rainfall is measured within 15 minutes of 0830 hr (IST) everyday. AWS daily rainfall is calculated by

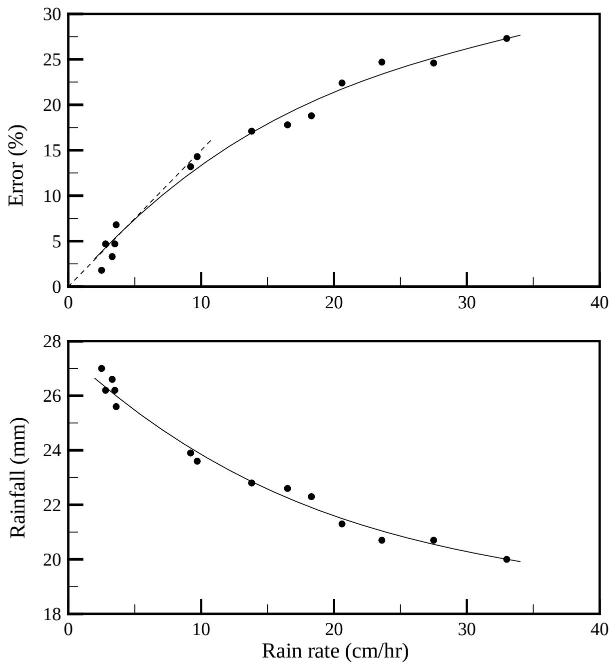

Fig. 7. Dependence of the total amount of rainfall measured by the tipping bucket raingauge on rain rate (bottom), and the corresponding error (top). The actual amount of total rainfall during each trial is 27.5 mm

accumulating the 10 minute interval rains for the preceding 24 hours and ending at 0830 hr (IST). The agreement between the amounts of rainfall from the two raingauges is good, however, there are also few occasions where the differences are significant. This is more clearly seen in the scatter plot of AWS *versus* IMD rainfall shown in Fig. 5. For Vengurla and Honnavar, the points are scattered along the line of equal rainfall and no systematic bias is observed, whereas, for Karwar, IMD rain gauge rainfall tends to be on the higher side.

We do not expect AWS and IMD daily rainfall values to exactly match on all days for several reasons other than inherent instrument differences which can be reduced by the calibration. Firstly, IMD measures rainfall every day at 0830 hr (IST), but the actual time of observation may vary by about 15 minutes on either side of this time. AWS rainfall corresponds to that during the previous 24 hours ending at 0830 hr (IST) exactly. If it was raining at the time of observation [Figs. 6(a&b), which also shows typical rainfall patterns during IREs], then a difference in the times of taking the readings can contribute to difference in the measured rainfall amounts. In this case, if AWS rainfall is more on a given day compared to that of IMD's, then we expect it to be lower than that of IMD's on the next day and *vice versa*. Such a trend is clearly seen in Vengurla data, but not that clearly at Honnavar and Karwar. Differences in the heights of rain gauge openings and any obstacles nearby can also contribute to the difference in the measured rainfall by bring about differences in the wind circulation around the rain gauges. Another important parameter is the rate of rainfall. The construction of the present tipping bucket rain gauge is such that rain falling over an area of 200 cm^2 is made to accumulate in a small cup which tilts when 2 ml of water is collected (corresponds to 0.1 mm rainfall). There are two cups and the position of the tilted cup is taken by the empty one, and this changeover takes a finite time. If the rainfall is continuous, then a fraction of the rain water goes into the cup that is undergoing tilting. The amount of water lost depends on the rain rate (RR) and the rainfall measured by the tipping bucket rain gauge is expected to decrease with RR.

In order to quantify the error arising from the rain rate, experiments were carried out in which an exactly known quantity of water (550 ml, corresponds to 27.5 mm total rainfall) was discharged into the tipping bucket rain gauge at different flow rates. The measured cumulative rainfall along with its percentage error are shown in Fig. 7 as a function of RR. Total amount of rainfall measured decreases with increasing rain rate and the dependence is nonlinear. At rain rates of less than 10 cm hr^{-1}, the percentage error in the measured rainfall (e) is approximately given by,

$$e = 100^* (R_0 - R)/R_0 = 1.4^* RR, \quad (1)$$

where R_0 is the actual amount of rainfall, R is the measured rainfall, and RR is specified in cm hr^{-1}. Fig. 7 shows that unless corrected, the rain rate can be a major source of error in the rainfall measured by the tipping bucket rain gauge. Repeating the experiment at a given RR several times (~5 in the present study) showed that the differences in the measured rainfall among these runs are within experimental errors. Thus, by knowing the RR, we can apply corrections to get the actual rainfall. In fact, the AWS rainfall shown in Figs. 4(a-c) & Fig. 5 are with rain rate corrections.

Correcting for rain rate and discounting for the possible difference in rainfall measuring timings could not account for the large differences between the AWS and IMD daily rainfall amounts on many days at Karwar Figs. 4(a-c). It was observed by the IMD personnel at Karwar (who went to the site to take synoptic observations) that on some days, rain water would accumulate in the open collector area of the AWS rain gauge instead of discharging into the cups below. Bird menace was responsible for this. Karwar IMD observatory is on the beach with a fish market and a garbage dumping place in its immediate neighborhood. Many birds are around and sometime they drop small pieces of grass

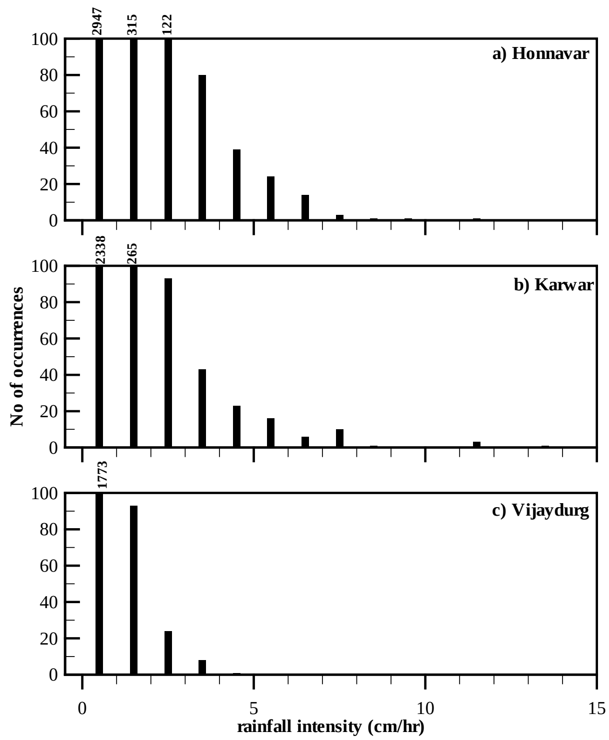

Figs. 8(a-c). Histogram of rainfall intensities. Numbers at the top of the bars show the number of occurrences in cases where the values exceeded the maximum scale on the *y*-axis

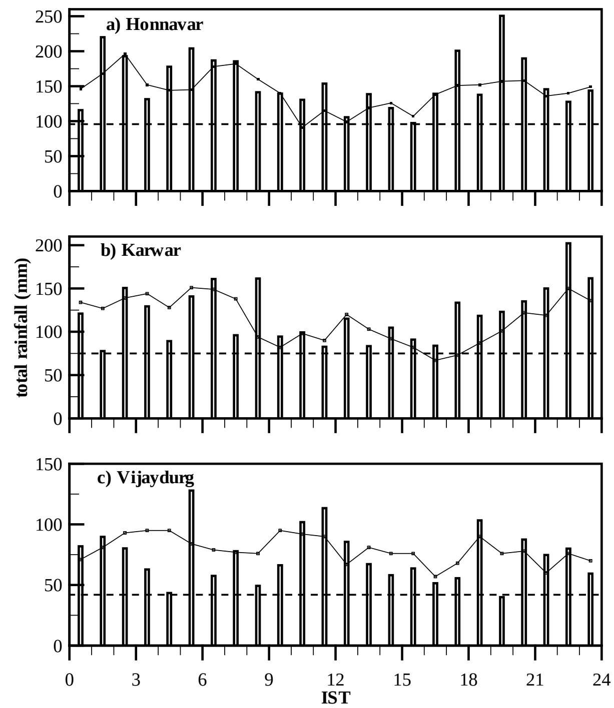

Figs. 9(a-c). Total amount of rainfall received during different times of the day. Dashed line is drawn to indicate the minimum amount of rainfall. The solid line with dots shows the number of times rain was detected during the hour

and other objects on the rain gauge. These objects often cover the narrow hole in the rain gauge and water was not freely falling on the cups and sometime used to completely block the passage of water itself. When the block was removed, the accumulated water emptied rapidly into the cups resulting in incorrect amount of rainfall and its timing. The arrows in Figs. 6(a&b) show the time of rainfall measurement by IMD. A big spike in the AWS rainfall is observed around this time at Karwar on many days which is not that common at Honnavar. This is unlikely to be weather related. The bird menace problem is real and serious, but there is no simple procedure to estimate the error resulting from this.

For the first time automatic rain gauges have been operated at Honnavar, etc., and it is of interest to know the distribution of RR at these locations which are among the heaviest rainfall spots on the west coast. The histogram of RR at Honnavar, Karwar and Vijaydurg for the 2003 monsoon season are shown in Figs. 8(a-c). In this figure, the 10 minute interval rainfall (nonzero values only included) is converted to hourly rainfall by multiplying by a factor of 6 and the resulting RR values are binned in 1 cm hr^{-1} intervals. It is observed from Figs. 8(a-c) that RR was less than 1 cm hr^{-1} more than 83% of the time, and exceeded 10 cm hr^{-1} only twice at Honnavar and four times at Karwar. (The numbers at Karwar could be in error owing to the bird problem as already discussed.)

(*iii*) *Diurnal variation of rainfall*

Diurnal variation of rainfall and convection over India have been reported previously (Prasad 1970, Rao and Rao 1993). It varies from place to place and also marginally depend on the month as well (Prasad 1970). To find out the nature of diurnal variations at the present AWS locations, the total amount of rainfall received at different hours during June-September 2003 along with the number of times it rained during these hours (which is proportional to the probability of rainfall) have been computed and shown in Figs. 9(a-c). At the three stations considered, the diurnal patterns of rainfall are different. At Honnavar, probability of rainfall is high between midnight and early morning and low between 10-15 hours (IST) and again increases after 19 hours. At Karwar, less rain is observed from 9–17 hours (IST) and more rainfall in late evening and early morning. (The peak between 0800 hr (IST) and 0900 hr (IST) at Karwar is likely to be an artificial one caused by the rain gauge blockage.) In contrast, noon hours are among preferred times of rainfall at Vijaydurg. It is also observed that higher probability of rainfall does not necessarily mean more rainfall during

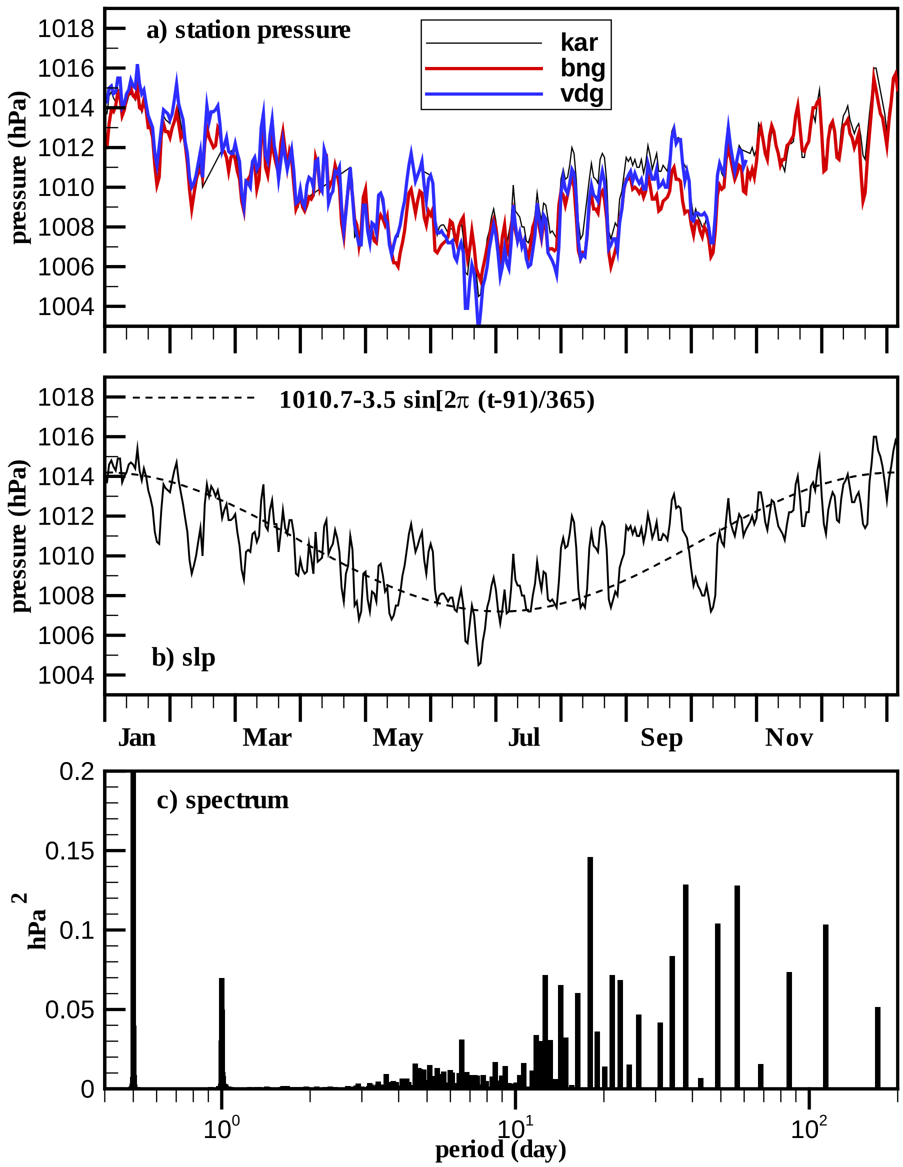

Figs. 10(a-c). (a) Time series of daily average surface pressure (reduced to sea level) at Karwar, Vijaydurg and Honnavar. (b) Reconstructed pressure time series and (c) Spectrum of the surface pressure using hourly data

the hour. For example, at Honnavar the highest probability of rainfall is between 0200 hr and 0300 hr (IST), whereas, the maximum rainfall is observed between 1900 hr and 2000 hr (IST).

(*iv*) *Intraseasonal variation*

The tropical atmosphere exhibits a strong variation on subseasonal time scales, and the 40-50 day Madden – Julian oscillation (Madden and Julian 1971) is a well known example. Here we consider the variation of surface pressure (reduced to sea level) over a period of one year. (Results and discussions to follow will reveal why pressure is considered here.) Fig. 10(a) shows the variation of sea level pressure (SLP) at Karwar, Vijaydurg and Bangalore (at the Indian Institute of Science Bangalore, an AWS is being continuously operated since January 2003). A remarkable feature observed in Fig. 10(a) is that despite the large spatial separation, the surface pressure variations are almost identical at the three stations. Only on few occasions (when synoptic systems developed), differences are noticeable. Another prominent

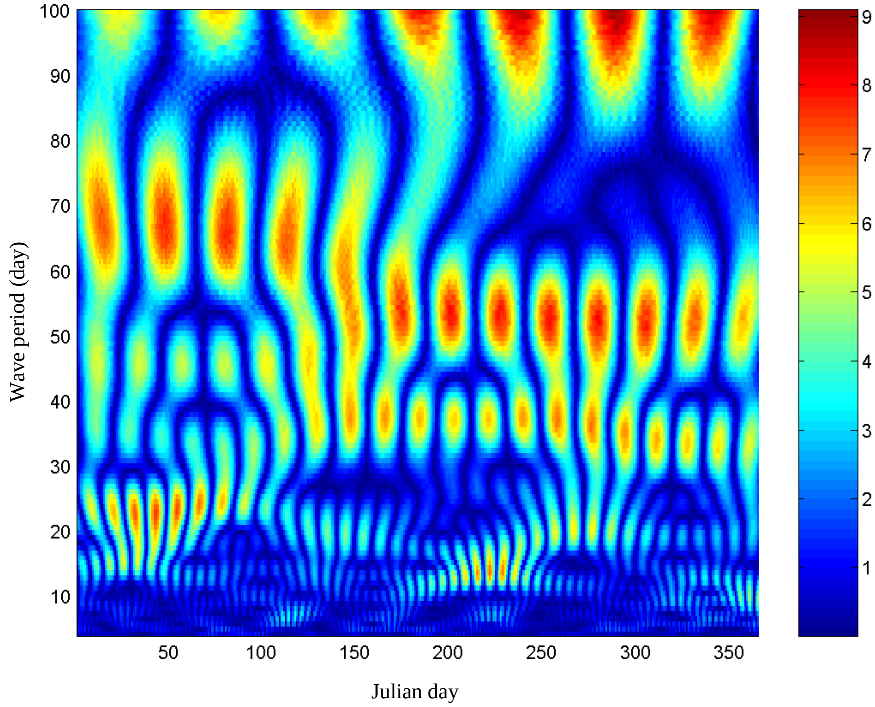

Fig. 11. Wavelet transform of the surface pressure time series. Absolute values of wavelet coefficients are shown as function of time and wave period

feature is the oscillations in the pressure on different time scales, from super synoptic to subseasonal throughout the year (and not just limited to monsoon months). It is possible to get more precise information on the dominant subseasonal time scales by taking the Fourier transform of the time series. There are data gaps at each station, but it so happens that they are at different times at the three stations, and it is possible to construct a continuous time series by combining pressure data from the three stations without incurring serious errors (the same cannot be said about variables such as wind speed and rainfall). Here Karwar pressure is taken as the reference pressure and missing data is filled from that of the nearest station's where SLP is available (in the order of Honnavar, Vijaydurg and Bangalore). The SLP so constructed is shown in Fig. 10(b). It is observed that an annual cycle is present in the SLP pressure with an amplitude of 3.5 hPa. The spectrum of the reconstructed hourly SLP (after removing the annual cycle) is shown in Fig. 10(c). The strongest variation is on the semidiurnal time scale and there is some energy on the diurnal scale. Notice a minor peak on synoptic time scale (between 6 and 7 days), but the longer time scales (2-3 weeks and more than 4 weeks) dominate the pressure variations.

It is observed from Fig. 10(b) that longer time periods are dominant during the winter months and variations around biweekly time scales are prominently seen during the summer monsoon period. One limitation of the Fourier transform approach to extracting time scales is that it gives an average picture for the entire data period, and does not tell when these events occurred. The wavelet transform gives more precise information about the timing of the different modes and their relative importance. In Fig. 11, the absolute values of the wavelet coefficients obtained using a Morlet wavelet are shown as a function of time and wave period. A clear separation of time scales is observed in Fig. 11. During January and February, the most dominant mode has 60-70 day period and the second mode has a period around 23 days. During March-April, the dominant mode is again 60-70 day one, but the second mode shifts to a higher period (~40 days). During the monsoon period and in the following season, the dominant mode has a period between 50 and 60 days and the next prominent mode has period between 30 and 40 days. A biweekly mode is observed during July-August which diminishes in strength during November-December.

4. Concluding remarks

As part of the ARMEX programme, AWSs have been successfully installed and operated at Honnavar, Karwar, Vengurla and Vijaydurg. The present study provides a glimpse of the kind of data set that results from the operation of AWSs. Some important observations based on the analysis of the data collected at these places are as follows.

(*i*) The air temperature exhibits properties typical of tropical climate with the amplitudes of annual cycle comparable to that of the diurnal cycle.

(*ii*) About 83% of the time, the rate of rainfall is less than 1 cm hr^{-1} and those exceeding 10 cm hr^{-1} are very rare.

(*iii*) Diurnal influence is clearly seen in rainfall, with early morning and late evening times preferred compared to noon hours at Karwar and Honnavar, while at Vijaydurg, noon time is one of the preferred times of rainfall.

(*iv*) The surface pressure exhibits variations on different time scales well separated from each other. The most dominant mode has 60-70 day period during January-March, whereas it shifts to 56-60 day period after May, during which period 30-40 day mode is also prominently seen.

Acknowledgements

This work is supported by a grant from the Department of Science and Technology, New Delhi, Govt. India and we thank the agency. We thank the Director General of Meteorology, India Meteorological Department for the permission and encouragement to set up AWSs at IMD observatories in Honnavar and Karwar. We thank Dr. B. P. Patil, Director, Regional Fruit Research Station Vengurla for providing the facilities to set up and operate AWSs at Vengurla and Vijaydurg, Shri U. D. Hegde, Shri Ramesh and Shri Bingarde for their help in running the AWSs and Mrs. L. Kiranmayi for the wavelet analysis of pressure time series data.

References

Bhat, G. S. and Ameenulla S., 2000, “Surface meteorological instrumentation for BOBMEX”, *Proc. Indian Acad. Sci., (Earth Planet. Sci.)*, **109**, 221-227.

Madden, R. A. and Julian, P., 1971, “Detection of a 40-50 day oscillation in the zonal wind”, *J. Atmos. Sci*., **28**, 702-708.

Prasad, B., 1970, “Diurnal variation of rainfall in India”, *Indian J. Met. Geophys.*, **21**, 443-450.

Rao, A. V. R. K. and Rao, V. R., 1993, “Diurnal variation of cloudiness during southwest monsoon season using INSAT-1B radiance data”, *Mausam*, **44**, 127-134.

Rao, Y. P., 1976, “Southwest monsoon”, India Meteorological Department, Meteorological Monograph Synoptic Meteorology, No. 1/1976, Delhi, p367.